Proteomic Characterization of Isolated Retinal Pigment Epithelium Microvilli*[S]

Vera L. Bonilha‡, Sanjoy K. Bhattacharya, Karen A. West, Jian Sun, John W. Crabb, Mary E. Rayborn, and Joe G. Hollyfield

Polarized epithelial cells are characterized by displaying compartmentalized functions associated with differential distribution of transporters, structural proteins, and signaling molecules on their apical and basolateral surfaces. Their apical surfaces frequently elaborate microvilli, which vary in structure according to the specific type and function of each epithelium. The molecular basis of this heterogeneity is poorly understood. However, differences in function will undoubtedly be reflected in the specific molecular composition of the apical surface in each epithelial subtype. We have exploited a method for isolating microvilli from the mouse eye using wheat germ agglutinin (WGA)-agarose beads to begin to understand the specific molecular composition of apical microvilli of the retinal pigment epithelium (RPE) and expand our knowledge of the potential function of this interface. Initially, apical RPE plasma membranes bound to WGA beads were processed for morphological analysis using known apical and basolateral surface markers. The protein composition of the apical microvilli was then established using proteomic analysis. Over 200 proteins were identified, including a number of proteins previously known to be localized to RPE microvilli, as well as others not known to be present at this surface. Localization of novel proteins identified with proteomics was confirmed by immunohistochemistry in both mouse and rat eye tissue. The data generated provides new information on the protein composition of the RPE apical microvilli. The isolation technique used should be amenable for isolating microvilli in other epithelia as well, allowing new insights into additional functions of this important epithelial compartment. ***Molecular & Cellular Proteomics 3:1119–1127, 2004.***

Epithelial cells are characterized by the asymmetric distribution of proteins and lipids in their plasma membrane: a basic feature referred to as polarity. The functional polarity of epithelial cells is dependent on the asymmetric distribution of specific enzymes, signaling molecules, and transport proteins between their apical and basolateral surface membranes (1). The apical surface of cuboidal and columnar epithelial cells commonly faces a luminal cavity and is characterized by the presence of numerous surface membrane elaborations referred to as microvilli. Microvilli greatly increase the apical surface area and, consequently, the number of transport and signaling proteins it contains, thereby enhancing the epithelial functional capacity. Absorptive epithelia such as kidney and intestine have their apical surface decorated with highly organized apical microvilli of uniform length and width. More dynamic and less organized structures are present in the epithelial cells of the placenta and the retinal pigment epithelium (RPE),[1] which perform endocytosis and phagocytosis, respectively. The basis of this morphological heterogeneity is poorly understood and is likely to be related to the specialized function and specific molecular composition of the microvilli in each epithelial cell type. A first step toward the understanding of the relationship between the structure and the functions of specialized epithelial surfaces is through the identification of their constituent molecules (2).

The RPE is a low-cuboidal epithelium containing very long sheet-like apical microvilli that project into a complex extracellular matrix, referred to as the interphotoreceptor matrix. At this surface, the microvilli interact with the tips of cylindrical photoreceptor outer segments extending from the outer retinal surface. The RPE basal surface is highly infolded and interacts with the underlying Bruch's membrane (3), an acellular layer separating the RPE from the choriocapillaris. The polarized organization of RPE cells is essential for the vectorial transport of the different molecules between the choriocapillaris and the neural retina and vice versa.

The RPE performs highly specialized, unique functions essential for homeostasis of the neural retina. These include phagocytosis of photoreceptors' shed outer segments, directional transport of nutrients into and removal of waste products from photoreceptor cells, and visual pigment transport and regeneration. The apical microvilli of the RPE play a key role in mediating these activities (3–5). Another unique characteristic of the RPE is the "reversed polarity" of proteins such as the Na,K-ATPase pump, EMMPRIN, and the adhesion molecule N-CAM at the apical surface, rather than at the basolateral surface where these proteins are found in other epithelia (6–9). However, the RPE shares many of the com-

From The Cole Eye Institute, Department of Ophthalmic Research, The Cleveland Clinic Foundation, Cleveland, OH 44195

Received, August 9, 2004, and in revised form, September 10, 2004
Published, MCP Papers in Press, September 14, 2004, DOI 10.1074/mcp.M400106-MCP200

[1] The abbreviations used are: RPE, retinal pigment epithelium; WGA, wheat germ agglutinin (*Triticum vulgaris*) lectin; Glut-1, glucose transporter type 1; integrin αv, vitronectin receptor α subunit; EBP50, ERM-binding phosphoprotein 50.

mon characteristics of other transporting epithelia such as the presence of antioxidative enzymes, amino peptidase (7), and the glucose transporter (10, 11) in their apical microvilli.

A more complete definition of the protein composition of the RPE apical microvilli should provide additional insight into other biochemical processes that occur at this interface that are important for the support and maintenance of vision. To this end, we isolated RPE microvilli using wheat germ agglutinin (WGA)-agarose beads (12) and defined the protein composition using of MS. Several new proteins identified in this compartment were confirmed with immunocytochemistry.

EXPERIMENTAL PROCEDURES

Isolation and Protein Identification of Intact RPE Apical Microvilli—RPE microvilli were isolated using the protocol initially described by Cooper (12) with the addition of the mechanical removal of the retina after enzymatic digestion. This procedure was recently described in detail (5) and is only briefly summarized here. C57Bl6 mice were sacrificed by CO_2 asphyxiation, and the eyes were enucleated. The anterior segments were removed and the eyecups with the exposed neural retina were incubated in 320 U/ml bovine testes hyaluronidase (Sigma, St. Louis, MO) in Hank's buffered solution for 1h at 37 °C. The neural retina was peeled off from the RPE. Eyecups were extensively washed with TBS plus 1 mM $CaCl_2$ for 1 h at 4 °C followed by incubation with WGA-agarose beads (Sigma) in TBS for 2–3 h at 4 °C. WGA beads were gently scrapped from the eyecups, collected into eppendorf tubes, washed extensively with TBS, and processed for biochemical, morphological, or immunohistochemical analysis. For proteomics analyses, the beads were dissolved in 2× Laemmli buffer, boiled, and resolved by SDS-PAGE on 4–15% gradient gels (Bio-Rad, Hercules, CA). The gel lanes were cut from top to bottom into ~2-mm slices. Gel slices were washed, reduced, alkylated, digested with trypsin, extracted, and resultant peptides subjected to LC MS/MS analysis using a QTOF2 mass spectrometer equipped with a CapLC System (Waters Corp., Milford, MA). Protein identifications from MS/MS data utilized the Swiss-Prot, and the NCBI sequence databases and the search engines Protein Lynx TM Global server and Mascot (Matrix Science, London, United Kingdom) (5, 13, 14).

Morphological Characterization of the Isolated Microvilli—For quality control of the isolation methods, samples of the WGA-agarose beads with attached microvilli and bead-treated eyecups were fixed in 2.5% glutaraldehyde in 0.1 M cacodylate buffer, sequentially dehydrated in ethanol and embedded in Epon as previously reported (15). Thin sections were prepared and electron micrographs were taken on a Tecnai 20 200-kV digital electron microscope (Philips, Hillsboro, OR) using a Gatan image filter and digital camera at 3,600 diameters and are printed at identical magnifications. Additional WGA beads with attached intact microvilli were fixed in 4% paraformaldehyde made in PBS, permeabilized in 0.2% Triton X-100 made in PBS for 10 min at room temperature, and reacted with antibodies to specific apical and basolateral domain markers. Samples were observed under an epifluorescence microscope, and images were collected with a cooled CCD camera (Hamamatsu C5810). Image panels were composed using AdobePhotoshop 5.5 (Adobe, San Jose, CA).

Immunocytochemistry of Identified Apical Microvilli Proteins—To confirm the localization of some of the proteins identified by LC MS/MS analysis, immunohistochemical assays were performed using both paraffin and cryosections of rats and mice eyes. Eyes were enucleated and fixed by immersion in 4% paraformaldehyde made in PBS for 3 h at 4 °C, subsequently the anterior segments were removed. For paraffin processing, fixed eyecups were dehydrated and embedded in paraffin. Immunostaining was carried out on 12-μm sections. After deparaffinization and rehydration to PBS, sections were subjected to heat-mediated antigen retrieval by pressure cooking in 10 mM citric acid buffer, pH 6.0. For cryosectioning, eyecups were fixed as described above, quenched with 50 mM NH_4Cl made in PBS for 1 h at 4 °C, infused successively with 15 and 30% sucrose made in the same buffer and with Tissue-Tek "4583" (Miles Inc., Elkhart, IN). For labeling, sections were blocked in PBS supplemented with 0.3 mM $CaCl_2$, 1 mM $MgCl_2$, and 1% BSA (PBS/CM/BSA) for 30 min, and incubated with the monoclonal anti-neuroglycan C antibody in PBS/CM/BSA overnight at 4 °C. The sections were washed in PBS/CM/BSA and incubated with secondary antibodies coupled to Alexa 488 and Alexa 594 (Molecular Probes, Eugene, OR) for 1 h at room temperature. Cell nuclei were labeled with 1 μM TO-PRO-3 (Molecular Probes) in PBS for 15 min. A series of 1-μm *xy* (*en face*) sections were collected using a laser scanning confocal microscope (Leica TCS-SP, Exton, PA). Each individual *xy* image of the retinas stained represents a three-dimensional projection of the entire cryosection (sum of all images in the stack). Polyclonal antibody to Lumican was a generous gift from Chia-Yang Liu (Bascom Palmer Eye Institute, Miami, FL) and used at 1:500. Monoclonal antibody to rat neuroglycan C (BD Biosciences Pharmingen, San Diego, CA) was used at 2.5 μg/ml. Phalloidin-FITC (Sigma) was used at 0.5 μg/ml.

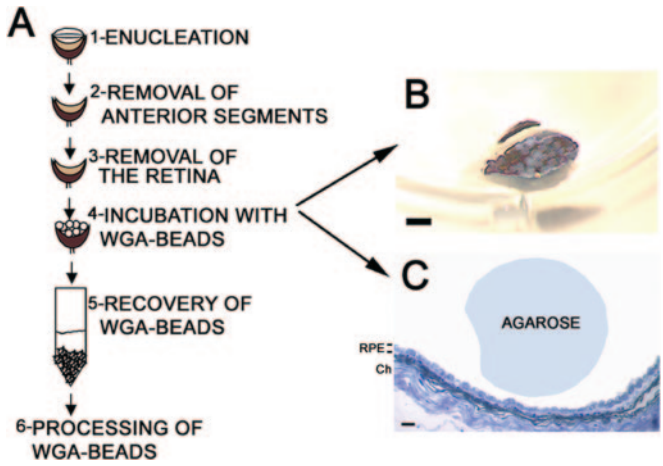

FIG. 1. **Microvillar isolation scheme.** *A*, *lane 1*, mouse eyes are enucleated; *lane 2*, the anterior segments are surgically removed; *lane 3*, the retina is removed after enzymatic treatment; *lane 4*, WGA-agarose beads are subsequently overlaid on the exposed RPE eyecups (*B*). Next, the WGA-beads are gently scraped from the eyecups, beads are collected into tubes, washed, and further processed for either biochemistry or morphology assays. For light microscopy analysis, eyecups with WGA beads were embedded in resin, and semithin sections were stained with toluidine blue (*C*). *Ch*, choroid. (*Bars*: *B*, 2 mm; *C*, 100 μm.)

RESULTS

RPE Microvilli Isolation—A schematic overview of the microvilli isolation method is presented in Fig. 1. The procedure relies on the interaction of *N*-acetylglucosamine and sialic acid-containing glycoconjugates present in abundance on the free surface of epithelial microvilli (12, 16) with the WGA lectin conjugated to the agarose beads. Mass interactions of the surface glycoconjugates with the immobilized lectin on the bead allow for the detachment of the RPE microvilli upon physical removal of the WGA beads. Analyzing the residual eyecups by transmission electron microscopy, we observed

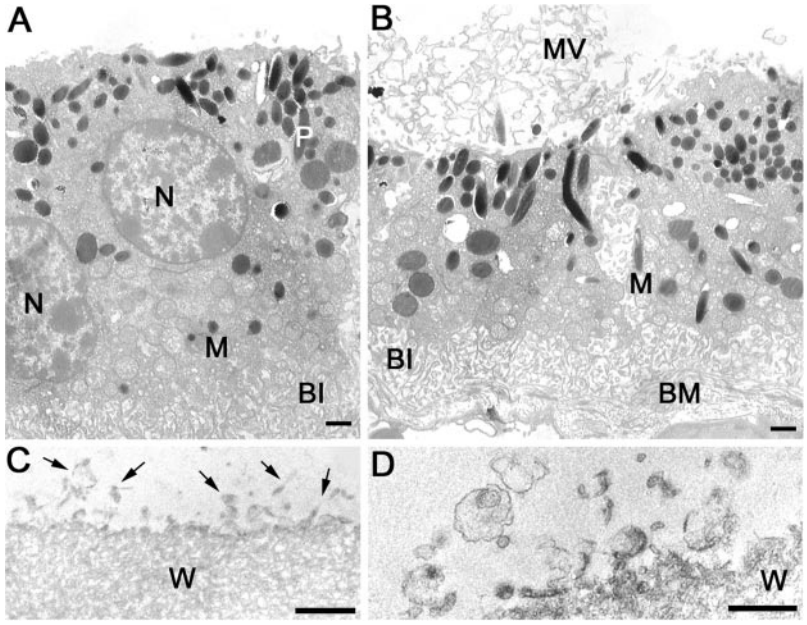

FIG. 2. **Transmission electron microscopy of mouse eyecups reacted with WGA-agarose beads (*A* and *B*) and the WGA beads scraped off the eyecups (*C* and *D*).** *A*, residual RPE cell deprived of microvilli but with an intact cytoplasm and basal infoldings still attached to the Bruch's membrane. *B*, most of the RPE cells had their microvilli removed by the WGA beads but some cells in the eyecup still have intact microvilli (MV). *C* and *D*, RPE Microvilli attached to WGA beads scraped from mouse eyecups (*arrows*). p, pigment; *BI*, basal infoldings; *M*, mitochondria; *N*, nucleus; *BM*, Bruch's membrane; *W*, WGA agarose beads. Electron micrographs were taken on a Tecnai 20, 200-kV digital electron microscope using a Gatan image filter and digital camera at 3,600 diameters and are printed at identical magnifications. (*Bars*: *A*, *B*, and *C*, 1 μm; *D*, 0.5 μm.)

that the RPE layer remains attached to the Bruch's membrane following the loss of its apical membranes (Fig. 2). The RPE cells that remained following the loss of their apical microvilli displayed normal ultrastructure without any significant damage to the cell body (Fig. 2, *A* and *B*). Some cells, however, retained their apical microvilli, demonstrating that not all the microvilli were extracted with this procedure (Fig. 2*B*). Subsequent analysis of the WGA beads showed extensive surface areas covered with microvilli (Fig. 2, *C* and *D*), indicating that this procedure allows for selective removal of apical microvilli from RPE layer.

The microvillar fraction while still attached to the WGA beads was also tested for RPE markers using antibodies directed to apical and basolateral proteins. The fixed beads were probed with specific antibodies and observed under an epifluorescence microscope. Fig. 3 shows that beads with microvilli are labeled with antibodies directed to the apical protein Na,K-ATPase (Fig. 3*A*) and with proteins present both in the apical and basolateral surfaces like ezrin (Fig. 3*B*) and glucose transporter type 1 (Glut-1) (Fig. 3*C*) but not with the basolateral marker, laminin (Fig. 3*D*). A punctate pattern characteristic of microvillar staining was observed. These data suggests that the WGA bead preparations provide a highly purified RPE microvilli fraction (Figs. 2 and 3), lacking significant cytoplasmic and basal protein contaminants.

When the isolated microvilli were subjected to fractionation on a gradient SDS-PAGE, they showed a distinctly different banding pattern compared with total RPE lysates (Fig. 4). The RPE microvilli fraction showed several prominent protein bands (ca. 280, 250, 210, 150, 88, and 49 kDa) that were not as prominent in the total RPE lysate (compare Fig. 4, *lanes 5* and *6*). In contrast, several major bands in the molecular mass range 33–85 kDa that were prominent in the total RPE lysate were missing in the microvilli fraction. None of these enriched proteins in the microvillar fraction were recovered under control conditions, including WGA bead alone (Fig. 4, *lane 4*) or protein A-agarose before (Fig. 4, *lane 2*) and after (Fig. 4, *lane 3*) exposure to eyecups.

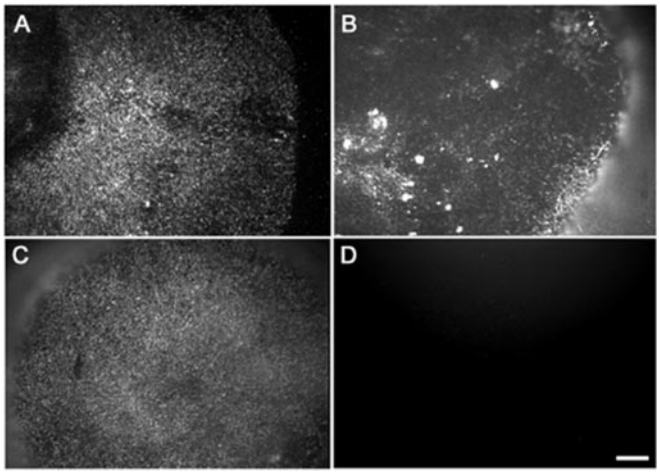

FIG. 3. **Morphological characterization of microvilli-enriched fraction.** WGA beads scraped off the mouse eyecups were washed, fixed in 4% paraformaldehyde, permeabilized with 0.2% Triton X-100, and immunoprobed with antibodies to Na,K-ATPase (*A*), ezrin (*B*), Glut-1 (*C*), and laminin (*D*). Positive staining displayed a punctate pattern, characteristic of microvilli localization, when WGA beads were reacted with antibodies specific to proteins known to be present in the RPE apical microvilli but not with a known basolateral protein. (*Bar*: 100 μm.)

Identification of RPE Microvillar Protein—MS of peptides present in SDS-PAGE following in-gel trypsin digestion resulted in identification of 283 proteins (Supplemental Table I). A summary of selected proteins identified is shown in Table I.

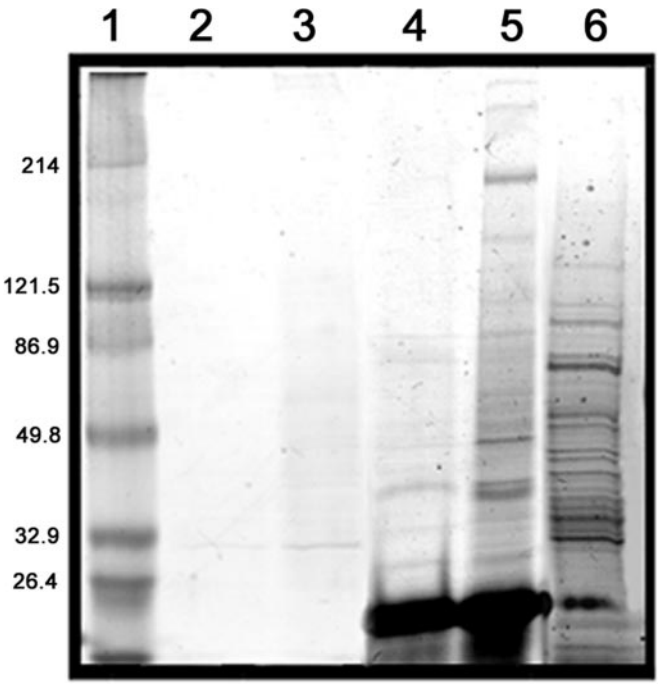

FIG. 4. **Coomassie blue-stained SDS-PAGE gels of RPE microvilli-enriched fraction.** RPE microvilli fraction and total RPE lysates were subjected to SDS-PAGE and stained with Coomassie blue. A representative gel is shown. *Lane 1*, molecular mass markers; *lane 2*, protein A-agarose beads; *lane 3*, protein A-agarose beads incubated with mouse eyecups; *lane 4*, WGA-agarose beads without incubation with mouse eyecups; *lane 5*, purified RPE microvilli proteins (~10 μg) recovered from WGA-agarose beads after incubation with 16 mouse eyecups; *lane 6*, mouse RPE whole-cell lysate (~10 μg).

The identified protein profile of the RPE microvilli can be divided into different functional categories: retinoid-metabolizing, cytoskeletal, enzymes, extracellular matrix components, membrane proteins and transporters, unknown, and others (Fig. 5). Several proteins identified in the RPE microvilli fraction were previously identified in the microvilli of other epithelial cells. A number of identified RPE microvilli proteins has been shown independently to localize to this compartment, including basigin, Glut-1, vitronectin receptor α subunit (integrin αv), Na,K-ATPase, ezrin, and ERM-binding phosphoprotein 50 (EBP50). In contrast, proteins resident to the basolateral domain like laminin, ZO-1, and SAP-97 were not found in these samples, substantiating the validity that this isolation procedure allows preferential enrichment of RPE apical microvilli. These results therefore provide an unbiased account of proteins present in the apical microvilli.

Many extracellular molecules were identified in this preparation, which were not characterized as being present in the RPE microvilli-interphotoreceptor matrix. Localization of lumican and neuroglycan C in adult mouse and rat eye sections was investigated to gain further understanding of the distribution of these proteins. Lumican was detected by immunofluorescence of cryosections of mouse eyecups at the RPE apical and basal surfaces and around the photoreceptor outer segments (Fig. 6*A*). Lumican localization greatly overlapped with the phalloidin-FITC staining of actin filaments (Fig. 6*B*), as demonstrated by the yellow color in merged images (Fig. 6*C*). Similarly, rat paraffin sections probed with neuroglycan C antibody revealed localization in association with both the RPE apical and basal surfaces and the photoreceptor outer segment layers (Fig. 6, *D–F*). Our data suggests that some of the new extracellular components identified with this method are indeed localized to the interphotoreceptor matrix, which is isolated along with the apical microvilli.

DISCUSSION

This report describes a simple and efficient method that produces a highly enriched RPE microvilli fraction. This conclusion is supported by several observations. First, we provide morphological evidence for specific removal of microvilli from cells that remain otherwise intact and for association of microvilli with the isolated beads. Second, we show the presence of known apical markers in the microvilli-enriched fraction, whereas there was absence of basolateral. Third, MS analysis allowed the identification of novel proteins confirmed to be present on the apical surface through subsequent morphological analysis of the tissue.

This method produces a fraction of intact microvilli characterized by the presence of proteins such as annexin A2 (17, 18), annexin A5 (19), α-enolase and creatine kinase B (20), phosphoglycerate kinase (21), cytosolic malate dehydrogenase (22), lactate-dehydrogenase (23), GST (20, 24, 25), catalase (24), peroxiredoxin (26), among others previously shown to localize to epithelia microvilli.

Epithelia involved in the net transport of ions such as sodium, chloride, and calcium are highly susceptible to the reactive oxygen species generated by the ion transport process itself. As a consequence, epithelial cells evolved mechanisms to protect themselves from these reactive molecules (27, 28). The presence of several antioxidant enzymes observed in our intact microvilli fraction is consistent with this hypothesis.

The method described here may find application in unraveling both basic mechanisms and pathological conditions in all epithelial microvilli. Examples of pathologies involving epithelial microvilli include microvillus inclusion disease and chronic placental insufficiency. Microvillus inclusion disease is a congenital enteropathy of intractable diarrhea. Both the molecular defect and the pathophysiology of this disease are unclear, but its main feature includes villus atrophy, loss of microvilli, and the presence of intracytoplasmic inclusions, vacuoles containing brush-border-like microvilli called microvilli inclusions (29). More recently, it has been shown that decreased expression of apical membrane transporters such as NHE-2, NHE-3, and sodium glucose transporter is observed in microvillus inclusion disease samples (30). Chronic

TABLE I
Selected proteins identified on WGA beads after incubation with apical RPE

Proteins	Accession no.[a]	Peptides matched	Function[b]	Experiment[c]		
Actin, cytoplasmic 1 (β-actin)	P60710	11	CYT	+		+
Actin, γ	Q9QZ83	19	CYT	+	+	+
α enolase	P17182	5	E	+	+	+
Annexin A2	P07356	2	MT	+		
Annexin A5	P48036	3	MT	+		
β enolase	*P13929*	3	E	+	+	
Basigin	P18572	6	MT	+	+	+
Carbonic anhydrase XIV	Q9WVT6	2	E		+	
Chloride intracellular channel 6	Q96NY7	2	MT	+	+	+
Cellular retinaldehyde-binding protein (CRALBP)	Q9Z275	6	RM	+	+	+
Cytokeratin 15	*I49595*	5	CYT	+	+	+
Decorin	P28654	4	ECM		+	+
Dermcidin	P81605	3	ECM	+		
EBP50	Q9JJ19	1[d]	CYT	+		
Ezrin	P26040	4	CYT		+	+
Fibromodulin	P50608	4	ECM		+	+
Fructose-bisphosphate aldolase A	P05064	4	E	+	+	+
Glut-1	*P17809*	3	MT	+	+	+
GST P	*P04906*	2	E		+	
Glyceraldehyde 3-phosphate dehydrogenase	P16858	8	E	+	+	+
Glycogen phosphorylase	Q9WUB3	5	E		+	+
Interphotoreceptor retinoid-binding protein (IRBP)	P49194	5	RM	+	+	+
L-lactate dehydrogenase A chain (LDH)	P06151	3			+	
Lumican	P51885	9	ECM	+	+	+
Malate dehydrogenase	P14152	2		+		+
Membrane-associated adenylate kinase	Q9R0Y4	2	MT		+	
Moesin	P26041	3	CYT	+	+	
Monocarboxylate transporter 1	*AAC13720*	3	MT	+	+	+
Monoglyceride lipase	O35678	2	E		+	+
Na,K-transporting ATPase α1 chain	P06685	6	MT	+	+	+
Neuroglycan C	Q9QY32	1[c]	ECM		+	
Neuronal membrane glycoprotein M6-a	P51674	1	MT			+
Peroxiredoxin 1	Q63716	1[c]	E			+
Peroxiredoxin 2	Q9CWJ4	2	E		+	
Phosphoglycerate kinase	P09411	2	E		+	+
Profilin I	P10924	2	CYT		+	
Pyruvate kinase, M1 isozyme	P14618	4	E	+		
Pyruvate kinase, M2 isozyme	P52480	2	E		+	
Retinol-binding protein, cellular (CRBP)	Q00915	5	RM	+	+	
Retinol dehydrogenase, 11-cis (RDH5)	Q27979	3	RM	+	+	+
Sodium/potassium-transporting ATPase α-1	P06685	6	MT	+	+	+
Spectrin β chain	Q00963		CYT		+	+
Tubulin α-2 chain	P05213	6	CYT		+	+
Undulin 1	A40970	7	ECM		+	+
Vitronectin receptor α subunit (integrin αv)	P43406	3	MT		+	+
Total[e]				86	97	100

[a] Swiss-Prot database and NCBI (in italics) accession numbers are shown; for links use the EXPASY server at us.expasy.org/sprot/ and www.ncbi.nlm.nih.gov/entrez/query.fcgi?db=protein&cmd=search&term=.

[b] Functions: CYT, cytoskeleton and cytoskeleton-associated; E, enzyme; ECM, extracellular matrix; MT, plasma membrane and transporter; RM, retinoid metabolizing.

[c] WGA-coated beads were incubated on the apical RPE surface in mouse eyecups, recovered, washed, and bound proteins identified as described in the text. Selected results from three experiments are shown from 16 mouse eyes each.

[d] The identified peptide sequences: EBP50, AVDPDSPAEASGLR; peroxiredoxin 1, GLFIIDDKGILR; neuroglycan C, ETGSAIEAEELVR.

[e] Total of proteins identified by LC MS/MS and bioinformatics in each preparation.

placental insufficiency is characterized by cytotrophoblast microvilli pathology (31).

Another application for this method can be the identification of age-related changes in epithelia microvilli. Aging studies have shown a decrease in both the number and the length of epithelial microvilli and a declined function of plasma membrane enzymes and receptors (32–35). Specifically, the decrease in the activity of some of the enzymes

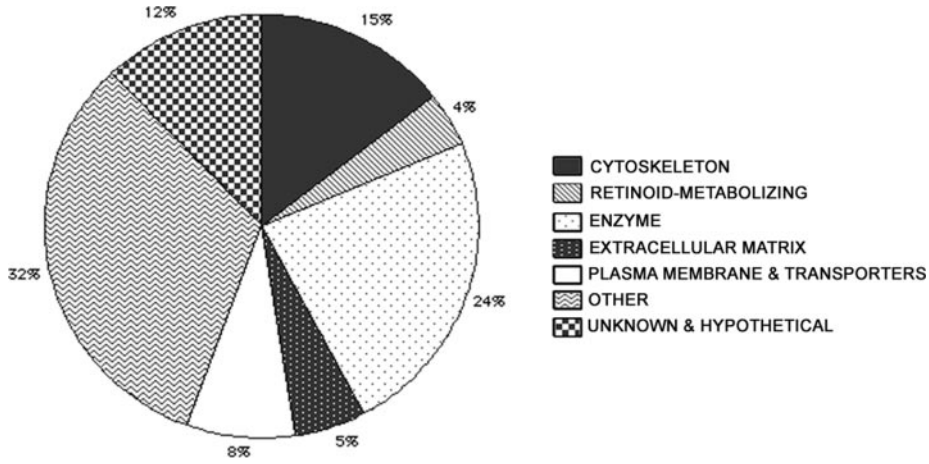

FIG. 5. **Functional characterization of proteins identified in mouse RPE microvilli.** Overall profile of functional categories of the proteins identified from mice RPE microvilli.

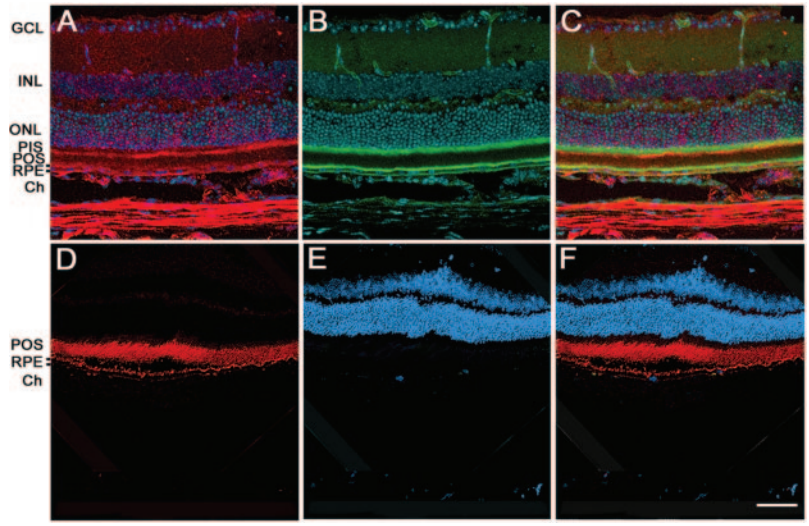

FIG. 6. **Tissue localization of lumican and neuroglycan C.** Twelve-micrometer cryosections of mouse eyes (*A* to *C*) were labeled with antibodies specific to lumican (*A*) and phalloidin-FITC (*B*). Overlapping of the staining in the RPE apical and basolateral surface is shown in yellow (*C*). Rat eye sections were labeled with anti-neuroglycan C (*D*). Cell nuclei were labeled with TO-PRO-3 (*E*). Merged images (*F*) showed that neuroglycan C localizes both to the photoreceptor outer segments (POS) and the RPE apical and basolateral surfaces. Sections were analyzed using a Leica laser scanning confocal microscope (TCS-SP2; Leica, Exton, PA). Each individual image of the retinas stained represents a three-dimensional projection of a series of 1-μm *xy* (*en face*) sections. *Ch*, choroid; *PIS*, photoreceptor inner segments; *ONL*, outer nuclear layer; *INL*, inner nuclear layer; *GCL*, ganglion cell layer. (*Bar*: 40 μm.)

detected in RPE microvilli like Na,K-ATPase, lactate-dehydrogenase, GST, phosphoglycerate kinase, adenylate kinase (36), and catalase has been established in various epithelia (23, 37, 38).

The RPE microvillar structure has not been extensively studied. However, some of the information available indicates that RPE microvilli possess an internal core bundle of densely packed actin filaments (39, 40). Further studies detected myosin VIIa at the base of apical processes (41, 42) but failed to detect villin, fimbrin, and myosin I (43, 44). The entire length of the RPE microvilli has been shown to contain ezrin and EBP50 (15, 43, 45–47). Moesin expression was previously detected in rat primary RPE cultures but not in RPE *in vivo* (15). Our proteomic study identified various types of actin and tubulin, β-spectrin, ezrin, moesin, EBP50, and profilin in the RPE microvilli-enriched fraction.

Our results are in agreement with previous studies that detected Na,K-ATPase (6, 48), Glut-1 (49, 50), monocarboxylate transporter (11), carbonic anhydrase (51), basigin (52, 53), EBP50 (46, 47), the vitronectin receptor (54), and the chloride intracellular channel 6 (55) in the RPE apical microvilli. However, proteins such as peropsin, Kir7.1, and organic anion transport protein 2, known to localize to RPE microvilli, were not identified in our study. This may be due to the fact that some of these proteins elute on one-dimensional SDS-PAGE with other proteins like enolase, tubulin, actin, and keratins, and their presence becomes masked after proteolysis by more abundant peptides, as previously reported (5). A previ-

ous study identified 278 proteins in normal adult human RPE lysates through cell fractionation and excision of two-dimensional SDS-PAGE gel spots (14). Forty-five of these proteins were also observed in the present analysis of mouse RPE apical microvilli. However, the previous study relied on the manual selection of the protein spots to be processed for MS.

Recently, an interaction was described between cellular retinaldehyde-binding protein and EBP50 in RPE microsomes (47). Our proteomic analyses was notably enriched in several retinoid-processing proteins such as cellular retinaldehyde-binding protein, 11-*cis*-retinol dehydrogenase, cellular retinol-binding protein 1, interphotoreceptor retinoid-binding protein, EBP50, and ezrin. These results were used to support the hypothesis of existence of a visual cycle protein complex in the RPE apical microvilli (5).

Lumican and fibromodulin, members of the small leucine-rich proteoglycan (SLRP) gene family (56), were detected for the first time in the RPE microvilli. Both proteins display overlapping expression patterns. Lumican is the major keratan sulfate proteoglycan present in the cornea. Cornea transparency is dependent on the highly ordered lattice-like collagen fibril architecture, which is dependent on lumican (57). Previous studies failed to detect lumican mRNA in retinas of newly born and adult mice (58). However, recent data generated in lumican-fibromodulin double-null mice reported multiple areas of retinal detachment (59). These retinal detachments were credited to the increased ocular axial length and biomechanical weakness due to the collagen fibril-matrix defects of the lumican-fibromodulin double-null mice. The presence of both lumican and fibromodulin in the RPE apical microvilli may also indicate a role for these molecules in stabilizing the attachment of the retina to the RPE.

Neuroglycan C is a transmembrane chondroitin sulfate proteoglycan that is predominantly expressed in the central nervous system (60). RPE and the retinal neuronal cells originate from the same optic vesicle in embryonic stage. A study reported the presence of neuroglycan C in the nerve fiber layer and inner plexiform layer in the postnatal developing rat retina (61). Besides, the presence of neuroglycan C was suggested both in the RPE apical microvilli and basal infoldings but not in the photoreceptor outer segments. Our study detected neuroglycan C in the RPE apical and basal surface and in the outer segments of photoreceptor cells. This apparent discrepancy in the detection of neuroglycan C in the photoreceptor outer segments might be related to differences in tissue processing and antibody antigenicity. The presence of this proteoglycan in both the RPE and photoreceptor outer segments suggests that it may be a component of the interphotoreceptor matrix present between both cell types.

In summary, our morphological and biochemical data shows a rapid, reliable, and reproducible method for generating enriched RPE microvilli without significant cytoplasmic or basal membrane contamination. This method together with an unbiased proteomic approach has the potential of differentially identifying disease-linked proteins affecting RPE and other epithelia.

Acknowledgments—We thank Wouter van't Hof and Josephine Adams for critical reading this manuscript.

* This work was supported by National Institutes of Health Grants EY06603, EY14239, and EY014240, a Research Center Grant from the Foundation Fighting Blindness, a grant from the National Glaucoma Research Program of American Health Assistance Foundation (G2004-047 to S. K. B.), funds from the Cleveland Clinic Foundation, and a NEI infrastructure grant (EY015638). The costs of publication of this article were defrayed in part by the payment of page charges. This article must therefore be hereby marked "*advertisement*" in accordance with 18 U.S.C. Section 1734 solely to indicate this fact.

S The on-line version of this manuscript (available at http://www.mcponline.org) contains supplemental material.

‡ To whom correspondence should be addressed: Department of Ophthalmic Research, The Cleveland Clinic Foundation, The Cole Eye Institute, 9500 Euclid Avenue, Cleveland, OH 44195. Tel.: 216-445-7690; Fax: 216-445-3670; E-mail: bonilhav@ccf.org.

REFERENCES

1. Rodriguez-Boulan, E., and Nelson, W. J. (1989) Morphogenesis of the polarized epithelial cell phenotype. *Science* **245,** 718–725
2. Arpin, M., Crepaldi, T., and Louvard, D. (1999) Cross-talk between apical and basolateral domains of epithelial cells regulates microvillus assembly, in *Epithelial Morphogenesis in Development and Disease* (Birchmeier, W., and Birchmeier, C., eds) pp. 95–116, Harwood Academic, Amsterdam, The Netherlands
3. Zinn, K. M., and Benjamin-Henkind, J. V. (1979) Anatomy of the human retinal pigment epithelium, in *The Retinal Pigment Epithelium* (Zinn, K. M., and Marmor, M. F., eds) pp. 3–31, Harvard University Press, Cambridge, MA
4. Bok, D. (1993) The retinal pigment epithelium: A versatile partner in vision. *J. Cell Sci. Suppl.* **17,** 189–195
5. Bonilha, V. L., Bhattacharya, S. K., West, K. A., Crabb, J. S., Sun, J., Rayborn, M. E., Nawrot, M., Saari, J. C., and Crabb, J. W. (2004) Support for a proposed retinoid-processing protein complex in apical retinal pigment epithelium. *Exp. Eye Res.* **79,** 419–422
6. Clark, V. M. (1986) The retina: A model for cell biology, Part II, in *The Cell Biology of the Retinal Pigment Epithelium* (Adler, R., and Farber, D., eds) pp. 129–167, Academic Press, New York
7. Gundersen, D., Orlowski, J., and Rodriguez-Boulan, E. (1991) Apical polarity of Na,K-ATPase in retinal pigment epithelium is linked to a reversal of the ankyrin-fodrin submembrane cytoskeleton. *J. Cell Biol.* **112,** 863–872
8. Gundersen, D., Powell, S. K., and Rodriguez-Boulan, E. (1993) Apical polarization of N-CAM in retinal pigment epithelium is dependent on contact with the neural retina. *J. Cell Biol.* **121,** 335–343
9. Marmorstein, A. D., Finnemann, S. C., Bonilha, V. L., Rodriguez-Boulan, E. (1998) Morphogenesis of the retinal pigment epithelium: Toward understanding retinal degenerative diseases. *Ann. N. Y. Acad. Sci.* **857,** 1–12
10. Almers, W., and Stirling, C. (1984) Distribution of transport proteins over animal cell membranes. *J. Membr. Biol.* **77,** 169–186
11. Bergersen, L., Johannsson, E., Veruki, M. L., Nagelhus, E. A., Halestrap, A., Sejersted, O. M., and Ottersen, O. P. (1999) Cellular and subcellular expression of monocarboxylate transporters in the pigment epithelium and retina of the rat. *Neuroscience* **90,** 319–331
12. Cooper, N. G., Tarnowski, B. I., and McLaughlin, B. J. (1987) Lectin-affinity isolation of microvillous membranes from the pigmented epithelium of rat retina. *Curr. Eye Res.* **6,** 969–979
13. Crabb, J. W., Miyagi, M., Gu, X., Shadrach, K., West, K. A., Sakaguchi, H., Kamei, M., Hasan, A., Yan, L., Rayborn, M. E., Salomon, R. G., and Hollyfield, J. G. (2002) Drusen proteome analysis: An approach to the etiology of age-related macular degeneration. *Proc. Natl. Acad. Sci. U. S. A.* **99,** 14682–14687
14. West, K. A., Yan, L., Shadrach, K., Sun, J., Hasan, A., Miyagi, M., Crabb, J. S., Hollyfield, J. G., Marmorstein, A. D., and Crabb, J. W. (2003) Protein

database, human retinal pigment epithelium. *Mol. Cell. Proteomics* **2,** 37–49
15. Bonilha, V. L., Finnemann, S. C., and Rodriguez-Boulan, E. (1999) Ezrin promotes morphogenesis of apical microvilli and basal infoldings in retinal pigment epithelium. *J. Cell Biol.* **147,** 1533–1548
16. Roper, K., Corbeil, D., and Huttner, W. B. (2000) Retention of prominin in microvilli reveals distinct cholesterol-based lipid micro-domains in the apical plasma membrane. *Nat. Cell Biol.* **2,** 582–592
17. Hansen, G. H., Pedersen, J., Niels-Christiansen, L. L., Immerdal, L., and Danielsen, E. M. (2003) Deep-apical tubules: Dynamic lipid-raft microdomains in the brush-border region of enterocytes. *Biochem. J.* **373,** 125–132
18. Massey-Harroche, D., Mayran, N., and Maroux, S. (1998) Polarized localizations of annexins I, II, VI and XIII in epithelial cells of intestinal, hepatic and pancreatic tissues. *J. Cell Sci.* **111,** 3007–3015
19. Turnay, J., Olmo, N., Lizarbe, M. A., and von der Mark, K. (2001) Changes in the expression of annexin A5 gene during in vitro chondrocyte differentiation: Influence of cell attachment. *J. Cell. Biochem.* **84,** 132–142
20. Stierum, R., Gaspari, M., Dommels, Y., Ouatas, T., Pluk, H., Jespersen, S., Vogels, J., Verhoeckx, K., Groten, J., and van Ommen, B. (2003) Proteome analysis reveals novel proteins associated with proliferation and differentiation of the colorectal cancer cell line Caco-2. *Biochim. Biophys. Acta* **1650,** 73–91
21. Hong, S. J., Shin, J. K., Kang, S. Y., and Ryu, J. R. (2003) Ultrastructural localization of phosphoglycerate kinase in adult *Clonorchis sinensis*. *Parasitol. Res.* **90,** 369–371
22. Hanss, B., Leal-Pinto, E., Teixeira, A., Christian, R. E., Shabanowitz, J., Hunt, D. F., and Klotman, P. E. (2002) Cytosolic malate dehydrogenase confers selectivity of the nucleic acid-conducting channel. *Proc. Natl. Acad. Sci. U. S. A.* **99,** 1707–1712
23. Napoleone, P., Bronzetti, E., and Amenta, F. (1991) Enzyme histochemistry of aging rat kidney. *Mech. Ageing Dev.* **61,** 187–195
24. Coursin, D. B., Cihla, H. P., Oberley, T. D., and Oberley, L. W. (1992) Immunolocalization of antioxidant enzymes and isozymes of glutathione *S*-transferase in normal rat lung. *Am. J. Physiol.* **263,** L679–L691
25. Davies, S. J., D'Sousa, R., Philips, H., Mattey, D., Hiley, C., Hayes, J. D., Aber, G. M., and Strange, R. C. (1993) Localisation of alpha, mu and pi class glutathione *S*-transferases in kidney: comparison with CuZn superoxide dismutase. *Biochim. Biophys. Acta* **1157,** 204–208
26. Novoselov, S. V., Peshenko, I. V., Popov, V. I., Novoselov, V. I., Bystrova, M. F., Evdokimov, V. J., Kamzalov, S. S., Merkulova, M. I., Shuvaeva, T. M., Lipkin, V. M., and Fesenko, E. E. (1999) Localization of 28-kDa peroxiredoxin in rat epithelial tissues and its antioxidant properties. *Cell Tissue Res.* **298,** 471–480
27. Davis, W. L., Matthews, J. L., Shibata, K., Kipnis, M., Farmer, G. R., Cortinas, E., Meiyr, J. C., and Goodman, D. B. (1989) The immunocytochemical localization of superoxide dismutase in the enterocytes of the avian intestine: The effect of vitamin D3. *Histochem. J.* **21,** 194–202
28. Muse, K. E., Oberley, T. D., Sempf, J. M., and Oberley, L. W. (1994) Immunolocalization of antioxidant enzymes in adult hamster kidney. *Histochem. J.* **26,** 734–753
29. Phillips, A. D., Jenkins, P., Raafat, F., and Walker-Smith, J. A. (1985) Congenital microvillous atrophy: Specific diagnostic features. *Arch. Dis. Child* **60,** 135–140
30. Michail, S., Collins, J. F., Xu, H., Kaufman, S., Vanderhoof, J., and Ghishan, F. K. (1998) Abnormal expression of brush-border membrane transporters in the duodenal mucosa of two patients with microvillus inclusion disease. *J. Pediatr. Gastroenterol. Nutr.* **27,** 536–542
31. Milovanov, A. P., Fokin, E. I., and Rogova, E. V. (1995) Basic pathogenetic mechanisms of chronic placental insufficiency. *Arkh. Patol.* **57,** 11–16
32. Weisse, I. (1995) Changes in the aging rat retina. *Ophthalmic Res.* **27,** 154–163
33. Hirai, T., Kojima, S., Shimada, A., Umemura, T., Sakai, M., and Itakura, C. (1996) Age-related changes in the olfactory system of dogs. *Neuropathol. Appl. Neurobiol.* **22,** 531–539
34. Jang, I., Jung, K., and Cho, J. (2000) Influence of age on duodenal brush border membrane and specific activities of brush border membrane enzymes in Wistar rats. *Exp. Anim.* **49,** 281–287
35. Serot, J. M., Bene, M. C., and Faure, G. C. (2003) Choroid plexus, aging of the brain, and Alzheimer's disease. *Front. Biosci.* **8,** S515–S521
36. Kadlubowski, M., and Agutter, P. S. (1977) Changes in the activities of some membrane-associated enzymes during *in vivo* ageing of the normal human erythrocyte. *Br. J. Haematol.* **37,** 111–125
37. Teillet, L., Preisser, L., Verbavatz, J. M., and Corman, B. (1999) Kidney aging: Cellular mechanisms of problems of hydration equilibrium. *Therapie* **54,** 147–154
38. Schmucker, D. L., Thoreux, K., and Owen, R. L. (2001) Aging impairs intestinal immunity. *Mech. Ageing Dev.* **122,** 1397–1411
39. Drenckhahn, D., and Wagner, H. J. (1985) Relation of retinomotor responses and contractile proteins in vertebrate retinas. *Eur. J. Cell Biol.* **37,** 156–168
40. Vaughan, D. K., and Fisher, S. K. (1987) The distribution of F-actin in cells isolated from vertebrate retinas. *Exp. Eye Res.* **44,** 393–406
41. Hasson, T., and Mooseker, M. S. (1995) Molecular motors, membrane movements and physiology: Emerging roles for myosins. *Curr. Opin. Cell Biol.* **7,** 587–594
42. Liu, X., Vansant, G., Udovichenko, I. P., Wolfrum, U., and Williams, D. S. (1997) Myosin VIIa, the product of the Usher 1B syndrome gene, is concentrated in the connecting cilia of photoreceptor cells. *Cell Motil. Cytoskeleton* **37,** 240–252
43. Hofer, D., and Drenckhahn, D. (1993) Molecular heterogeneity of the actin filament cytoskeleton associated with microvilli of photoreceptors, Muller's glial cells and pigment epithelial cells of the retina. *Histochemistry* **99,** 29–35
44. Owaribe, K., and Eguchi, G. (1985) Increase in actin contents and elongation of apical projections in retinal pigmented epithelial cells during development of the chicken eye. *J. Cell Biol.* **101,** 590–596
45. Kivela, T., Jaaskelainen, J., Vaheri, A., and Carpen, O. (2000) Ezrin, a membrane-organizing protein, as a polarization marker of the retinal pigment epithelium in vertebrates. *Cell Tissue Res.* **301,** 217–223
46. Bonilha, V. L., and Rodriguez-Boulan, E. (2001) Polarity and developmental regulation of two PDZ proteins in the retinal pigment epithelium. *Invest. Ophthalmol. Vis. Sci.* **42,** 3274–3282
47. Nawrot, M., West, K., Huang, J., Possin, D. E., Bretscher, A., Crabb, J. W., and Saari, J. C. (2004) Cellular retinaldehyde-binding protein interacts with ERM-binding phosphoprotein 50 in retinal pigment epithelium. *Invest. Ophthalmol. Vis. Sci.* **45,** 393–401
48. Bok, D. (1982) Autoradiographic studies on the polarity of plasma membrane receptors in retinal pigment epithelial cells, in *The Structure of the Eye* (Hollyfield, J. G., ed) pp. 247–256, Elsevier, Amsterdam
49. Harik, S. I., Kalaria, R. N., Whitney, P. M., Andersson, L., Lundahl, P., Ledbetter, S. R., and Perry, G. (1990) Glucose transporters are abundant in cells with "occluding" junctions at the blood-eye barriers. *Proc. Natl. Acad. Sci. U. S. A.* **87,** 4261–4264
50. Takata, K., Kasahara, T., Kasahara, M., Ezaki, O., and Hirano, H. (1992) Ultracytochemical localization of the erythrocyte/HepG2-type glucose transporter (GLUT1) in cells of the blood-retinal barrier in the rat. *Invest. Ophthalmol. Vis. Sci.* **33,** 377–383
51. Wolfensberger, T. J., Mahieu, I., Jarvis-Evans, J., Boulton, M., Carter, N. D., Nogradi, A., Hollande, E., and Bird, A. C. (1994) Membrane-bound carbonic anhydrase in human retinal pigment epithelium. *Invest. Ophthalmol. Vis. Sci.* **35,** 3401–3407
52. Miyauchi, T., Kanekura, T., Yamaoka, A., Ozawa, M., Miyazawa, S., and Muramatsu, T. (1990) Basigin, a new, broadly distributed member of the immunoglobulin superfamily, has strong homology with both the immunoglobulin V domain and the beta-chain of major histocompatibility complex class II antigen. *J. Biochem.* **107,** 316–323
53. Miyauchi, T., Jimma, F., Igakura, T., Yu, S., Ozawa, M., and Muramatsu, T. (1995) Structure of the mouse basigin gene, a unique member of the immunoglobulin superfamily. *J. Biochem.* **118,** 717–724
54. Finnemann, S. C., Bonilha, V. L., Marmorstein, A. D., and Rodriguez-Boulan, E. (1997) Phagocytosis of rod outer segments by retinal pigment epithelial cells requires $\alpha_v\beta_5$ integrin for binding but not for internalization. *Proc. Natl. Acad. Sci. U. S. A.* **94,** 12932–12937
55. Mizukawa, Y., Nishizawa, T., Nagao, T., Kitamura, K., and Urushidani, T. (2002) Cellular distribution of parchorin, a chloride intracellular channel-related protein, in various tissues. *Am. J. Physiol. Cell Physiol.* **282,** C786–C795
56. Iozzo, R. V. (1999) The biology of the small leucine-rich proteoglycans. Functional network of interactive proteins. *J. Biol. Chem.* **274,** 18843–18846
57. Chakravarti, S., Petroll, W. M., Hassell, J. R., Jester, J. V., Lass, J. H., Paul,

J., and Birk, D. E. (2000) Corneal opacity in lumican-null mice: defects in collagen fibril structure and packing in the posterior stroma. *Invest. Ophthalmol. Vis. Sci.* **41,** 3365–3373
58. Ying, S., Shiraishi, A., Kao, C. W., Converse, R. L., Funderburgh, J. L., Swiergiel, J., Roth, M. R., Conrad, G. W., and Kao, W. W. (1997) Characterization and expression of the mouse lumican gene. *J. Biol. Chem.* **272,** 30306–30313
59. Chakravarti, S., Paul, J., Roberts, L., Chervoneva, I., Oldberg, A., and Birk, D. E. (2003) Ocular and scleral alterations in gene-targeted lumican-fibromodulin double-null mice. *Invest. Ophthalmol. Vis. Sci.* **44,** 2422–2432
60. Shuo, T., Aono, S., Matsui, F., Tokita, Y., Maeda, H., Shimada, K., and Oohira, A. (2004) Developmental changes in the biochemical and immunological characters of the carbohydrate moiety of neuroglycan C, a brain-specific chondroitin sulfate proteoglycan. *Glycoconj. J.* **20,** 267–278
61. Inatani, M., Tanihara, H., Oohira, A., Otori, Y., Nishida, A., Honjo, M., Kido, N., and Honda, Y. (2000) Neuroglycan C, a neural tissue-specific transmembrane chondroitin sulfate proteoglycan, in retinal neural network formation. *Invest. Ophthalmol. Vis. Sci.* **41,** 4338–4346